

Structure, Mobility, and Interface Characterization of Self-Organized Organic–Inorganic Hybrid Materials by Solid-State NMR

Susan M. De Paul, Josef W. Zwanziger,[†] Ralph Ulrich, Ulrich Wiesner,^{*,‡} and Hans W. Spiess*

Contribution from the Max-Planck Institut für Polymerforschung, Postfach 3148, D-55021 Mainz, Germany

Received December 21, 1998. Revised Manuscript Received April 9, 1999

Abstract: The local chemical environments, dynamic heterogeneities, and nature of the interface in structured organic–inorganic composites prepared from poly(isoprene-*b*-ethyleneoxide) block copolymers, (3-glycidyl-oxypropyl)trimethoxysilane, and aluminum *sec*-butoxide via a sol–gel process are characterized by solid-state NMR. Such composites self-assemble into the characteristic morphologies of block copolymer systems, with the inorganic component selectively swelling the poly(ethylene oxide) phases. Here it is shown that the local chemical structure of the aluminosilicate component is nearly unperturbed by addition of the block copolymer and that the combined aluminosilicate/poly(ethylene oxide) layer is significantly less mobile than the polyisoprene. Spin-diffusion measurements on a composite with lamellar morphology indicate that no significant (>1 nm thick) poly(ethylene oxide) interphase exists between the polyisoprene and poly(ethylene oxide)/aluminosilicate layers, and therefore, the inorganic and poly(ethylene oxide) phases are intimately mixed on a molecular level. Implications of these findings for the materials properties are discussed.

Introduction

Composite materials consisting of both inorganic and organic phases have the potential to lead to a wide range of new technologies since they can simultaneously combine the best features of oxides and polymers. Already they have found applications as diverse as contact lenses, waveguides, scratch-resistant coatings, data-storage devices, chemical filters, biosensors, electrolytes, and dental fillings.^{1,2}

Organic–inorganic composites can be formed using a variety of synthetic approaches. Sol–gel processes have been used to produce hybrids with morphologies ranging from isolated nanoparticles of one component in a matrix of the other component to interpenetrating networks of inorganic and polymeric materials.^{1–3} Often such composites lack long-range order. More structured hybrid materials have been synthesized by utilizing the self-assembly properties of organic surfactants under different reaction conditions.^{4,5} Such approaches typically lead to mesophases consisting of ordered arrangements of organic spheres (with diameters of 2 to 10 nm) surrounded by a polymerized silicate matrix (with a wall thickness of 8 to 9 Å). So far, these materials have primarily been used as precursors in the synthesis of mesoporous silicates, which have

important catalytic applications.⁶ However, they also may provide an insight into fundamental issues in biomineralization.^{7,8}

To increase the diversity of composite morphologies, alternative templates such as bacteria⁹ and polymeric surfactants¹⁰ have been examined. In addition, hybrids have been formed by intercalating organic molecules and polymers in layered silicates.^{11,12} However, the richness of the block copolymer phase diagram suggests the possibility of using the self-assembly of block copolymers to guide composite structure formation.^{13,14} Both new morphologies^{13,15} and larger length scales¹⁶ are possible with this approach. For instance, the use of a triblock copolymer has extended the scale of mesoporous systems to 30-nm pores and 3–6-nm walls.¹⁶

Recently, novel composites have been developed where poly-(isoprene-*b*-ethylene-oxide) (PI-*b*-PEO) phase-separated block copolymer was mixed with the alkoxides (3-glycidyl-oxypropyl)-trimethoxysilane (GLYMO) and aluminum *sec*-butoxide in a sol–gel process.¹³ Due to the hydrophilic nature of PEO, the

(6) Kresge, C. T.; Leonowicz, M. E.; Roth, W. J.; Vartuli, J. C.; Beck, J. S. *Nature* **1992**, 359, 710.

(7) Mann, S.; Ozin, G. A. *Nature* **1996**, 382, 313.

(8) Mann, S.; Burkett, S. L.; Davis, S. A.; Fowler, C. E.; Mendelson, N. H.; Sims, S. D.; Walsh, D.; Whilton, N. T. *Chem. Mater.* **1997**, 9, 2300.

(9) Davis, S. A.; Burkett, S. L.; Mendelson, N. H.; Mann, S. *Nature* **1997**, 385, 420.

(10) Bagshaw, S. A.; Prouzet, E.; Pinnavaia, T. J. *Science* **1995**, 269, 1242.

(11) Fukushima, Y.; Okada, A.; Kawasumi, A.; Kurauchi, T.; Kamigaito, O. *Clay Miner.* **1988**, 23, 27.

(12) Giannelis, E. P. *Adv. Mater.* **1996**, 8, 29.

(13) Templin, M.; Franck, A.; Du Chesne, A.; Leist, H.; Zhang, Y.; Ulrich, R.; Schädler, V.; Wiesner, U. *Science* **1997**, 278, 1795.

(14) Antonietti, M.; Göltner, C. *Angew. Chem., Int. Ed. Engl.* **1997**, 36, 910.

(15) Ulrich, R.; Du Chesne, A.; Templin, M.; Wiesner, U. *Adv. Mater.* **1999**, 11, 141.

(16) Zhao, D.; Feng, J.; Huo, Q.; Melosh, N.; Fredrickson, G. H.; Chmelka, B. F.; Stucky, G. D. *Science* **1998**, 279, 548.

* To whom correspondence should be addressed.

[†] Permanent Address: Department of Chemistry, Indiana University, Bloomington, IN 47405.

[‡] Present Address: Materials Science and Engineering, 329 Bard Hall, Cornell University, Ithaca, NY 14853-1501

(1) Schubert, U.; Hüsing, N.; Lorenz, A. *Chem. Mater.* **1995**, 7, 2010.

(2) Judeinstein, P.; Sanchez, C. *J. Mater. Chem.* **1996**, 6, 511.

(3) Chen, W.; Feng, H.; He, D.; Ye, C. *J. Appl. Polym. Sci.* **1998**, 67, 139.

(4) Monnier, A.; Schüth, F.; Huo, Q.; Kumar, D.; Margolese, D.; Maxwell, R. S.; Stucky, G. D.; Krishnamurthy, M.; Petroff, P.; Firouzi, A.; Janicke, M.; Chmelka, B. F. *Science* **1993**, 261, 1298.

(5) Huo, Q.; Margolese, D. I.; Ciesla, U.; Feng, P.; Gier, T. E.; Sieger, P.; Leon, R.; Petroff, P. M.; Schüth, F.; Stucky, G. D. *Nature* **1994**, 368, 317.

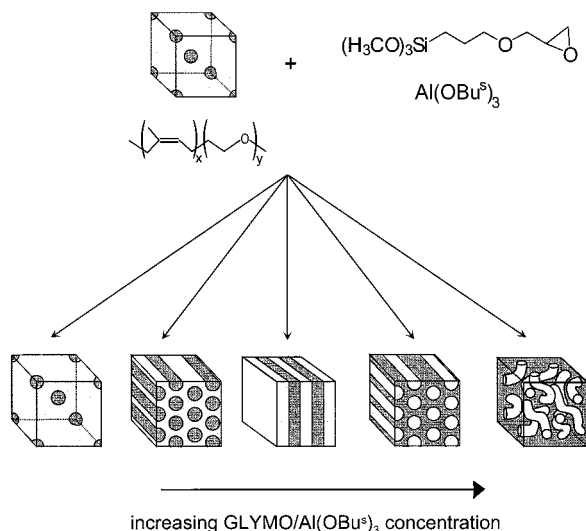


Figure 1. Schematic of PI-*b*-PEO/GLYMO/aluminum-*sec*-butoxide composite formation. The equilibrium structure of the pure block copolymer consists of a lattice of PEO spheres in a PI matrix. The radius of each PEO sphere is 3.5 nm, and the closest center-to-center distance between spheres is 15 nm. A hydrolyzed GLYMO/aluminum-*sec*-butoxide mixture is added in a sol-gel process and selectively swells the PEO phase. As the concentration of the alkoxide mixture is increased, the composite self-assembles into different morphologies: hexagonally packed cylinders of PEO/aluminosilicate, lamellae, hexagonally packed cylinders of polyisoprene, and, finally, disordered "wormlike" micelles of polyisoprene.

alkoxides selectively swelled this phase of the block copolymer, and the aluminum alkoxide served as a hardening component.¹⁷ By varying the concentration of the alkoxides, a range of nanoscale morphologies (spheres of PEO/aluminosilicate, hexagonally packed cylinders of PEO/aluminosilicate, lamellae, hexagonally packed cylinders of polyisoprene, and disordered polyisoprene "wormlike" micelles) could be formed (see Figure 1).¹⁵

While small-angle X-ray scattering (SAXS) and transmission electron microscopy (TEM) measurements enabled these morphologies to be characterized,^{13,15} many questions about the molecular-level nature of the mixing between the aluminosilicate phase and the PEO phase remained. In particular, the nature of the aluminosilicate/PEO-*b*-PI interface in the composite was unknown. In several other structured composite materials, the inorganic phase was shown to be stabilized by Coulombic interactions with either the organic template⁴ or with an intermediary counterion.⁵ For the aluminosilicate/PI-*b*-PEO system, however, the situation is quite different since the separation of inorganic and organic regions is not as clearly defined. GLYMO itself contains both inorganic and organic moieties, and the compatibility between GLYMO and PEO leads to a case where the organic polymer may significantly penetrate the inorganic network. This situation can be compared to that encountered in recent studies of an epoxy resin embedded in one phase of a block copolymer.^{18,19}

Possible models for the distribution of the aluminosilicate component in the PEO phase of the lamellar composite (see Figure 2) can be postulated by analogy to previously studied block copolymer/homopolymer systems.^{20–22} Theoretical studies of the addition of a homopolymer (A) to a block copolymer

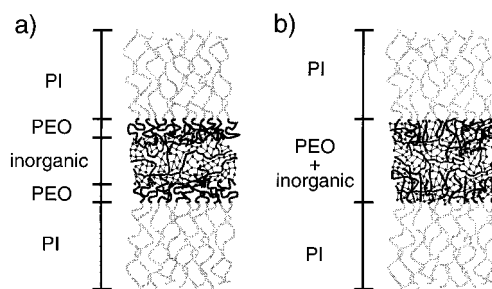


Figure 2. Two possible models for the distribution of the aluminosilicate network in the PEO phase of PI-*b*-PEO. (a) An interfacial layer, or interphase, of pure PEO is present. (b) The aluminosilicate network is distributed throughout the PEO phase.

(AB) suggest that two competing effects control the location of the homopolymer within one of the phases of a lamellar block copolymer.²³ Covalent links between the blocks tend to pull the A monomers of the block copolymer toward the B blocks (leaving the added homopolymer in the center of the A block), while entropic considerations favor a uniform distribution of the homopolymer throughout the A block. The size of the homopolymer tends to determine which scenario is most likely. When the molecular weight of the added homopolymer is large, the covalent effects dominate; when it is small, the entropic effects dominate. Such effects have been observed experimentally.²⁰

The hybrid aluminosilicate/PI-*b*-PEO system would be expected to behave similarly to such block copolymer/homopolymer systems since the aluminosilicate phase, which contains PEO-like organic segments, is selectively added to one block. However, the effective "size" of this aluminosilicate component is unknown. Two limiting scenarios are, therefore, possible. The first is that an interfacial layer of pure PEO lies between the PI and the PEO/aluminosilicate mixture (Figure 2a). In this case, PEO forms an interphase,²⁴ and three separate domains can be distinguished. The second possibility is that the aluminosilicate fully penetrates the PEO region of the block copolymer. Thus, there is no pure PEO layer, and the hybrid can adequately be described as a two-phase system (Figure 2b). Note that in both cases, the separation of the PI from the PEO is expected to be sharp (less than 5 Å) because of the inherent incompatibility of these two polymers.²⁵

The nature of the interface is closely linked with other structural and dynamical issues in this system. The hydrolysis of GLYMO and aluminum *sec*-butoxide alone (without the addition of a block copolymer) already forms an organic-inorganic composite, the local structure of which has been previously characterized.¹⁷ Condensation of the hydrolyzed GLYMO was shown to occur, producing a three-dimensional aluminosilicate network without long-range order. However, it is not known whether the addition of a block copolymer and the subsequent heat treatment would modify the local structure of the aluminosilicate network or whether the local structure would be sensitive to changes in concentration. Another open question is the issue of dynamic heterogeneities in the sample. The addition of inorganic components to the PEO phase would be expected to make the PEO more rigid. In fact, one common

(20) Hashimoto, T.; Tanaka, H.; Hasegawa, H. *Macromolecules* **1990**, *23*, 4378.

(21) Tanaka, H.; Hasegawa, H.; Hashimoto, T. *Macromolecules* **1991**, *24*, 240.

(22) Shull, K. R.; Winey, K. I. *Macromolecules* **1992**, *25*, 2637.

(23) Matsen, M. *Macromolecules* **1995**, *28*, 5765.

(24) Landfester, K.; Spiess, H. W. *Acta Polym.* **1998**, *49*, 451.

(25) Floudas, G.; Ulrich, R.; Wiesner, U. *J. Chem. Phys.* **1999**, *110*, 652.

(17) Templin, M.; Wiesner, U.; Spiess, H. W. *Adv. Mater.* **1997**, *9*, 814.

(18) Hillmyer, M. A.; Lipic, P. M.; Hajduk, D. A.; Almdal, K.; Bates, F. S. *J. Am. Chem. Soc.* **1997**, *119*, 2749.

(19) Lipic, P. M.; Bates, F. S.; Hillmyer, M. A. *J. Am. Chem. Soc.* **1998**, *120*, 8963.

reason for forming organic–inorganic composites is to improve the hardness of the polymeric materials.¹ It is unclear whether the PEO/aluminosilicate phase is uniformly rigidified or a distribution of mobilities exists.

Solid-state NMR spectroscopy can address many of these issues.^{26,27} Because it is sensitive to local chemical environments, it can be used to monitor changes in the aluminosilicate network (if any) as a function of composite morphology. It can also be used to probe local dynamics. Finally, by measuring the time scale of spin diffusion, length scales in heterogeneous samples, and therefore, the presence or absence of a pure PEO interphase, can be determined.^{24,28,29}

The purpose of this paper, therefore, is to characterize the local structures, the dynamic heterogeneities, and the nature of the organic–inorganic interface in composites made from PI-*b*-PEO, GLYMO, and aluminum *sec*-butoxide. It will be shown that the chemical structure of the aluminosilicate layer is essentially unperturbed by addition of the block copolymer. Information about relative mobilities in the lamellar sample will be provided by two-dimensional wideline separation (WISE).^{30,31} Finally, measurements of spin diffusion from the PI to the GLYMO will indicate that the PEO and aluminosilicate phases intimately mix and that no significant PEO interphase is present.

Experimental Section

The PI-*b*-PEO block copolymers were synthesized from commercial isoprene (Fluka) and ethylene oxide (Fluka) according to a recently published living anionic polymerization procedure.³² Two slightly different polymers were used to make the hybrids studied in this paper. The polymer used to form the lattice of PEO/aluminosilicate spheres and the hexagonally packed cylinders of PEO/aluminosilicate had a molecular weight of 15 200 g/mol, a polydispersity of 1.06, and a PEO volume fraction of 12%. The polymer used to form the other hybrids had a molecular weight of 14 200 g/mol, a polydispersity of 1.06, and a PEO volume fraction of 11%; samples formed from this polymer have been described in the literature.¹⁵ The structure of both copolymers is a lattice of spheres of PEO in a PI matrix.¹⁵ The organic–inorganic composite materials were formed in a sol–gel process from PI-*b*-PEO and various amounts of the inorganic precursors, (3-glycidyoxypropyl)-trimethoxysilane (GLYMO, see Figure 1 for the chemical structure) and aluminum *sec*-butoxide, as described in a previous paper.¹⁵ Small-angle X-ray scattering (SAXS) was used to determine the morphology of each composite, and the assignments were further verified by transmission electron microscopy (TEM).¹⁵ All morphologies depicted in Figure 1 were observed: a lattice of PEO/aluminosilicate spheres, hexagonally packed cylinders of PEO/aluminosilicate, lamellae, hexagonally packed cylinders of PI, and disordered “wormlike” micelles of PI.

Glass transition temperatures were measured by differential scanning calorimetry (DSC) on a Mettler DSC-30 over the temperature range –150 to 100 °C with a heating rate of 10 °C/min^{–1}.

One-dimensional ²⁷Al magic-angle spinning (MAS) and ¹H-to-²⁹Si cross-polarization (CP) MAS NMR spectra were recorded on a Bruker ASX-500 spectrometer with a ¹H frequency of 500.12 MHz, a ²⁷Al frequency of 130.32 MHz, and a ²⁹Si frequency of 99.35 MHz. The aluminum spectra were recorded at spinning speeds of 8–14 kHz using a small tip angle pulse (1 μs for $\gamma B_1/2\pi = 42$ kHz) and a recycle delay

(26) Engelhardt, G.; Michel, D. *High-Resolution Solid-State NMR of Silicates and Zeolites*; John Wiley and Sons Ltd.: Chichester, 1987.

(27) Schmidt-Rohr, K.; Spiess, H. W. *Multidimensional Solid-State NMR and Polymers*; Academic Press Ltd.: London, 1994.

(28) Clauss, J.; Schmidt-Rohr, K.; Spiess, H. W. *Acta Polym.* **1993**, *44*, 1.

(29) VanderHart, D. L. *Macromolecules* **1994**, *27*, 2837.

(30) Zumbulyadis, N. *Phys. Rev. B* **1986**, *33*, 6495.

(31) Schmidt-Rohr, K.; Clauss, J.; Spiess, H. W. *Macromolecules* **1992**, *25*, 3273.

(32) Allgaier, J.; Poppe, A.; Wilner, L.; Richter, D. *Macromolecules* **1997**, *30*, 1582.

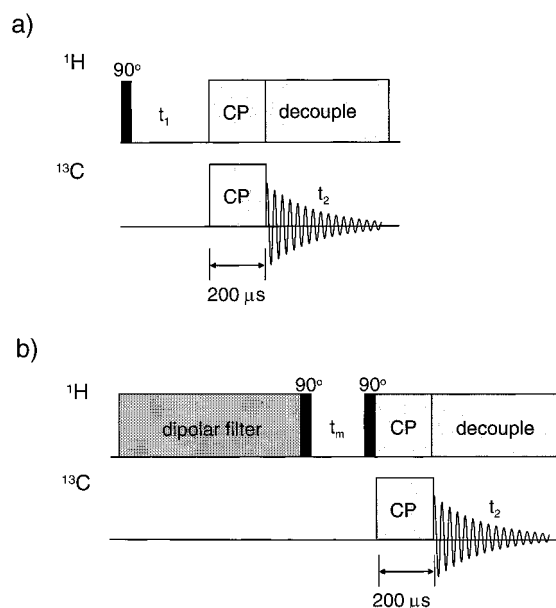


Figure 3. (a) Pulse sequence for the WISE experiment.^{30,31} The proton magnetization evolves for a time t_1 and is transferred to the carbons by cross polarization. The signal is subsequently detected. If the cross-polarization step is kept sufficiently short, the high-resolution carbon signals will be correlated with the dipolar-broadened signals of directly attached protons. Since the width of a proton line is a measure of molecular mobility, dynamic heterogeneities within the sample can be probed. (b) Pulse sequence for the carbon-detected proton spin diffusion experiment.^{33,34} A dipolar filter sequence (see Figure 4a) suppresses the magnetization from rigid regions of the sample. Magnetization from mobile protons “diffuses” to all other protons during the mixing time, t_m . The cross-polarization step allows specific sites to be monitored. Because the rate of spin diffusion is related to internuclear distances, domain sizes can be probed by monitoring changes in intensity as a function of mixing time.

of 100 ms. For the ¹H-to-²⁹Si CP/MAS experiments the 90° pulse length was 5 μs, the contact time was 2 ms, the recycle delay was 2 s, and the spinning speed was 4–5 kHz. Peak intensities were fitted using a deconvolution routine provided with the spectrometer software.

The high-resolution solid-state proton NMR spectrum was also obtained on the Bruker ASX-500 spectrometer. A spinning speed of 30 kHz was achieved with a commercial 2.5 mm MAS probe. The 90° pulse length was 3 μs, and the recycle delay was 3 s.

The wideline separation (WISE)^{30,31} (see Figure 3a) and dipolar filter spin diffusion measurements^{33,34} (see Figure 3b) were performed at a temperature of 268 K on a Bruker MSL-300 spectrometer. One-dimensional ¹H and ¹³C MAS as well as ¹H-to-¹³C CP/MAS experiments were also performed on this spectrometer. The ¹H Larmor frequency was 300.13 MHz, and the ¹³C Larmor frequency was 75.47 MHz. Typical 90° pulse lengths were 4 μs. The cross-polarization contact time was 200 μs, and the spinning speed was 4 kHz. Recycle delays for the ¹H-to-¹³C CP/MAS experiments were 2–3 s while recycle delays for the directly excited ¹³C MAS experiments were 30 s.

Figure 4a shows the multiple-pulse sequence used as a dipolar filter.^{33,35} In the limit of small interpulse spacings, τ , both chemical-shift and dipolar evolution are refocused, and the pulse sequence restores the system to its initial state (damped slightly by transverse relaxation). As the interpulse spacing increases, however, higher order terms start to reduce the efficiency of the refocusing. This effect is more pronounced for larger dipolar couplings. By choosing an intermediate value of τ (typically in the range of 10–20 μs), one can suppress the

(33) Egger, N.; Schmidt-Rohr, K.; Blümich, B.; Domke, W.-D.; Stapp, B. *J. Appl. Polym. Sci.* **1992**, *44*, 289.

(34) Cai, W. Z.; Schmidt-Rohr, K.; Egger, N.; Gerharz, B.; Spiess, H. W. *Polymer* **1993**, *34*, 267.

(35) Schmidt-Rohr, K. Diploma Thesis, Johannes Gutenberg University, Mainz, Germany, 1989.

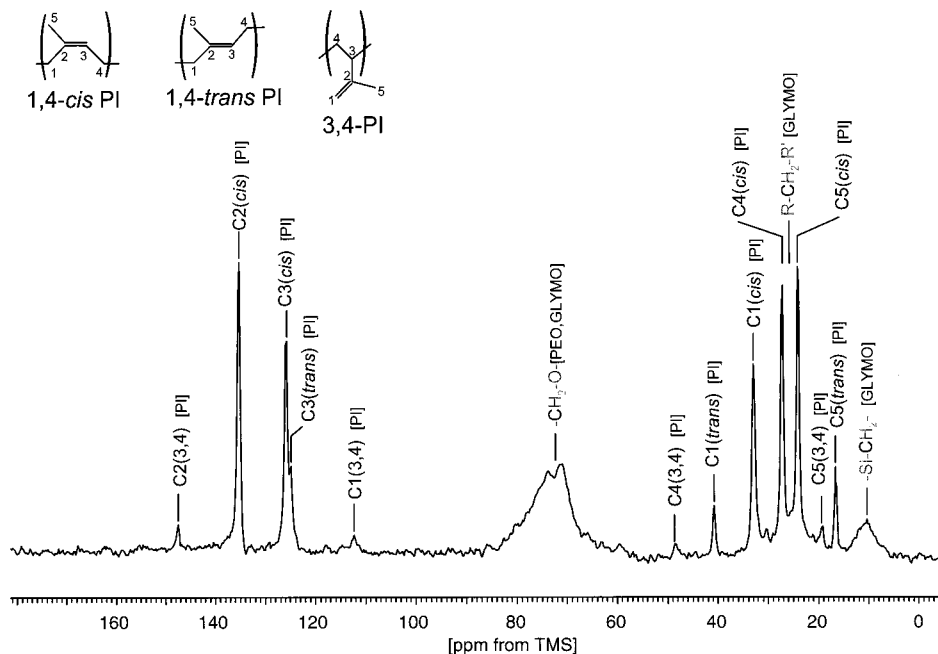


Figure 5. Room-temperature ^{13}C MAS spectrum of the composite consisting of hexagonally packed cylinders of polyisoprene (in a PEO/GLYMO/aluminum-*sec*-butoxide matrix). Five hundred and twelve scans with a recycle delay of 30 s were acquired. The narrow peaks are due to mobile polyisoprene ($T_g \approx 214$ K) in three different isomeric forms and are assigned according to the literature.⁴⁶ The broader peaks are due to PEO and hydrolyzed GLYMO as indicated in the figure. The spectra for all other composites show peaks in the same locations but with different intensities, as expected.

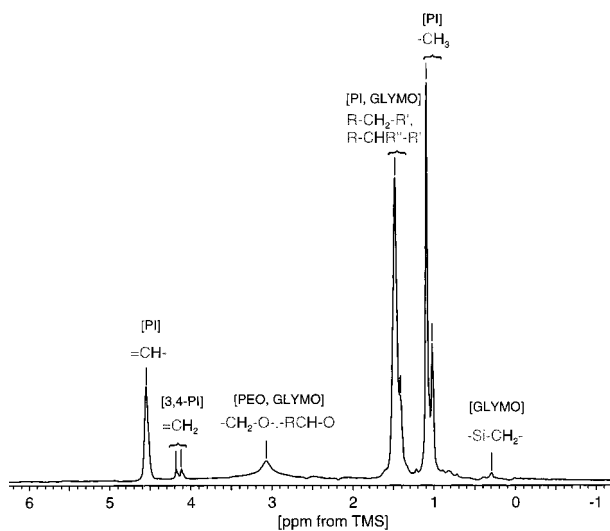


Figure 6. ^1H MAS spectrum of the lamellar composite obtained at a spinning speed of 30 kHz. Due to frictional heating from the fast sample spinning, the temperature was approximately 20 °C above room temperature.⁴⁷ Eight scans were recorded. Spectra were externally referenced using $\delta(^1\text{H}_2\text{O}) = 4.65$ ppm as an external reference. Peak assignments are based on solution-state spectra of pure GLYMO as well as known proton chemical shifts for PI and PEO.⁴⁶ In addition to the 1,4-polyisoprene which makes up the bulk of the PI phase of the block copolymer, a small amount of 3,4-polyisoprene is detectable. Although some hydroxy protons are expected to be present in the composite,^{17,41} their intensity would be significantly less than the $\text{Si}-\text{CH}_2-$ protons, and they are, therefore, undetectable.

Al) oxygens. Different T^n species resonate at different ppm values in a ^{29}Si NMR spectrum.⁸

Figure 7 shows the ^1H -to- ^{29}Si CP/MAS spectra of the hydrolyzed GLYMO/aluminum-*sec*-butoxide mixture, the lamellar composite, and the disordered micelles. Peaks due to T^1 , T^2 , and T^3 sites can be clearly distinguished in all three spectra. An additional downfield shoulder at -46.5 ppm is apparent in

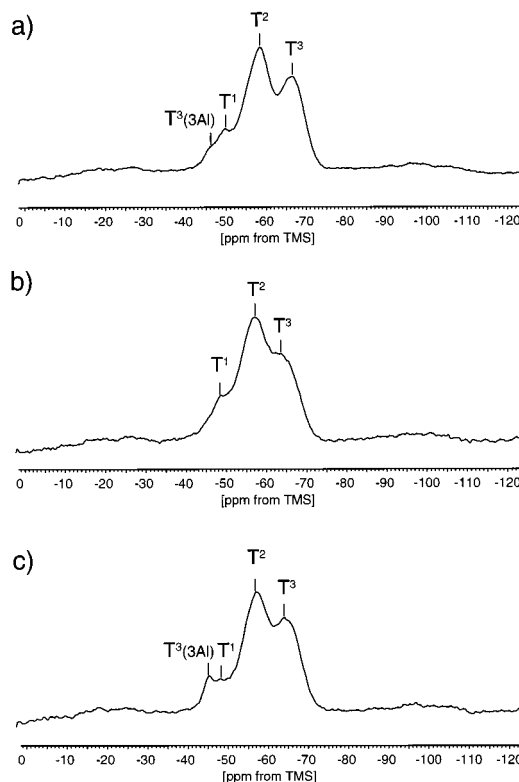


Figure 7. ^1H -to- ^{29}Si CP/MAS spectra of (a) the 80:20 GLYMO/aluminum-*sec*-butoxide mixture, (b) the lamellar composite, and (c) the disordered micelle composite. In all three spectra, peaks due to T^1 , T^2 , and T^3 sites are present. An additional downfield shoulder is present at -46.5 ppm in spectra (a) and (c) and is attributed to a T^3 site where the silicon atom is coordinated to three aluminums through bridging oxygens.¹⁷

the hydrolyzed mixture of GLYMO and aluminum *sec*-butoxide (Figure 7a). Such a peak has been observed previously in a study of hydrolyzed GLYMO/aluminum-*sec*-butoxide mixtures of

Table 1. Populations of Silicon and Aluminum Sites in Various Composite Materials

	silicon sites								aluminum sites	
	T ³ (3Al) ^a		T ¹ ^a		T ²		T ³		T _d %	O _h %
	[ppm]	% intensity	[ppm]	% intensity	[ppm]	% intensity	[ppm]	% intensity	intensity	intensity
80:20 GLYMO/Al(OBu) ³ b.c.c. lattice of spheres of PEO/aluminosilicate	-46.6	8	-50.3	16	-58.3	49	-66.5	35	45	55
hexagonal array of cylinders of PEO/aluminosilicate lamellae			-49.7	16	-57.8	50	-66.6	34	56	44
hexagonal array of cylinders of PI	-46.5	7	-50.3	6	-58.0	54	-66.4	33	50	50
disordered micelles of PI	-46.7	7	-50.5	5	-58.1	52	-66.2	35	47	53

^a Due to the proximity of the T³(3Al)¹⁷ and T¹ resonances, it was not always possible to deconvolve the two signals. In cases where deconvolution was not possible, the peak is listed at a T¹ site. However, this does not imply that no T³(3Al) sites are present in these samples.

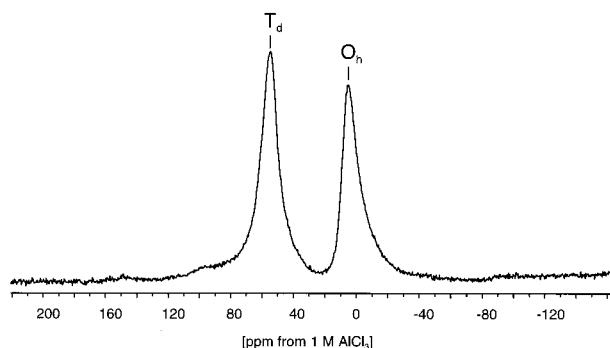


Figure 8. ²⁷Al MAS spectrum of the lamellar composite showing tetrahedrally and octahedrally coordinated aluminum in a 56:44 ratio. The spectrum was obtained with a short pulse (one-sixth of the solution 90° pulse) and a spinning speed of 12 kHz.

various concentrations¹⁷ and has been attributed to a specific T³ environment, RSi(OAl)₃, in which the silicon is coordinated via bridging oxygens to three aluminums. This peak is slightly more pronounced in the composites consisting of spheres of PEO/aluminosilicate, of hexagonally packed cylinders of polyisoprene, and of disordered polyisoprene micelles (see Figure 7c), but it is not separately resolved in the other two composites (see Figure 7b). Table 1 shows the results of fits of the ²⁹Si NMR spectra with Gaussian-shaped lines. The minimum number of lines necessary to obtain good agreement was used to fit each spectrum. Because cross polarization can lead to intensity distortions, these numbers should be viewed more as a basis for comparing the different samples rather than as a quantitative measurement of site populations. Nonetheless, since all silicon atoms are approximately the same distance from the nearest protons, intensity distortions are expected to be slight. When viewed as a whole, the populations of the various silicon environments do not significantly change as a function of composite morphology. In fact, the observed differences likely reflect normal fluctuations in the metal-alkoxide hydrolysis step.

Figure 8 shows the ²⁷Al MAS spectrum of the lamellar composite. Two peaks are visible, a peak due to octahedrally coordinated aluminum at 5.4 ppm and one due to tetrahedrally coordinated aluminum at 55.2 ppm. Both peaks are slightly asymmetric; the octahedral peak, in particular, has a significant upfield tail. The tetrahedrally coordinated aluminum can be assumed to be incorporated into the aluminosilicate lattice²⁶ while the octahedrally coordinated aluminum is attributed to aluminumoxohydroxo domains.¹⁷ Significantly, no peak is present in the 30–40 ppm region, which is where highly distorted tetrahedral sites would be expected to resonate. This indicates that there is not a significant number of severely distorted aluminum sites in the aluminosilicate network. The

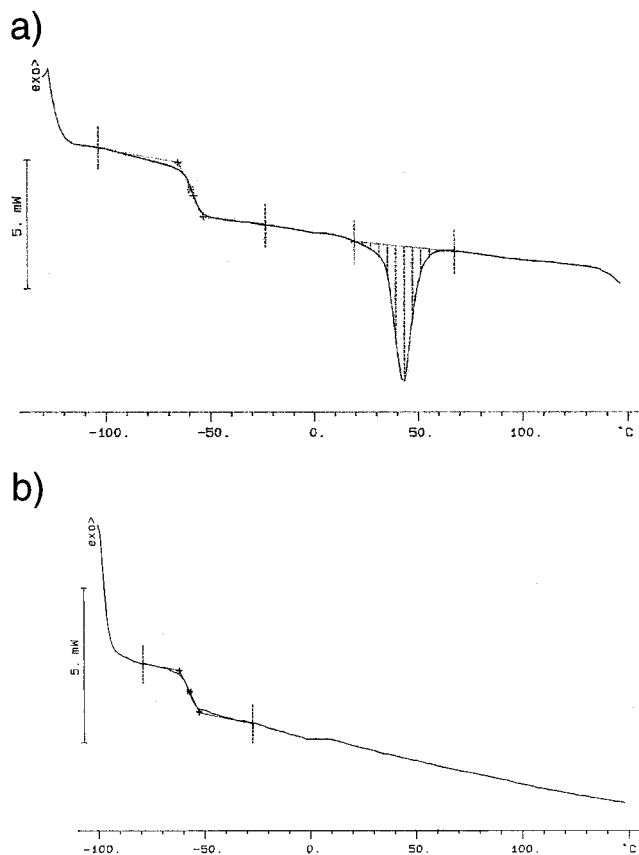


Figure 9. DSC traces of (a) the pure PI-*b*-PEO block copolymer and (b) the lamellar composite. The glass transition temperature of the PI in the composite ($T_g \approx 215$ K) is approximately unchanged from that of the bulk ($T_g \approx 214$ K). The DSC traces of all other composites look similar to (b). The concentration of PEO is too low to permit observation of its glass transition in any of the materials. Note that a melting peak at 315 K is clearly evident in the DSC of the pure block copolymer and indicates the presence of crystalline PEO; such a peak is absent from all of the composite materials.

spectra of the other samples (including the GLYMO/aluminum-*sec*-butoxide mixture without any block copolymer) are qualitatively similar to the spectrum of Figure 8, with peaks of the same shapes in the same positions. The relative intensities of the sites vary slightly from sample to sample, but no systematic relation to composite morphology is observed. These intensities (obtained by integration of the spectra) are also summarized in Table 1.

Additional indirect information about local structure is provided by differential scanning calorimetry. Figure 9 shows DSC traces for the pure block copolymer (Figure 9a) as well as the lamellar composite (Figure 9b). In both cases the DSC-

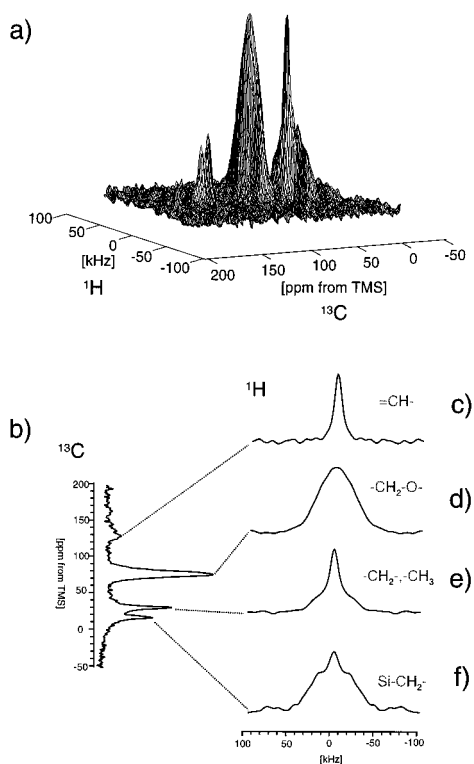


Figure 10. Results of a two-dimensional WISE experiment performed on the lamellar composite. (a) A stacked plot of the full spectrum. (b) The projection along the ^{13}C dimension. Proton slices corresponding to (c) the vinyl protons in PI, (d) the $-\text{CH}_2\text{O}-$ protons in PEO and GLYMO, (e) the aliphatic protons, found throughout the composite, which are not near oxygen or silicon, and (f) the $-\text{CH}_2-\text{Si}-$ protons in GLYMO. Larger proton line widths correspond to more rigid regions of the sample.

determined T_g values for polyisoprene are similar ($T_g \approx 214\text{--}215\text{ K}$); this is not surprising because the aluminosilicate is expected to reside only in the PEO block and not in the PI block.¹³ Unfortunately, the glass transition of PEO in these systems (expected to occur somewhere in the range $158\text{--}233\text{ K}$)³⁹ is too weak to be observed by DSC. However, a melting peak is clearly observed for the pure block copolymer at 315 K , which indicates the presence of crystalline PEO. Such a peak is absent from all of the composites.

Correlation of Structure and Mobility. 2D WISE Spectroscopy. While one-dimensional MAS and CP/MAS NMR provide information about the distributions of local sites in the composites, two-dimensional wideline separation spectroscopy (see Figure 3a) can give insight into the relative mobilities of different regions of the materials. Figure 10 shows the results of a WISE experiment performed on the lamellar composite at 268 K . (The sample was cooled to reduce the mobility of the polyisoprene so that cross polarization was possible.) Dramatic differences in mobility for the different regions of the sample were observed. The vinyl protons (which occur solely in polyisoprene) were quite mobile; the line width of the dipolar-broadened proton line was only 10.8 kHz . The least mobile protons were associated with the carbons adjacent to oxygen (found in poly(ethylene oxide) and GLYMO) and with the carbons adjacent to silicon (found exclusively in GLYMO). These line widths were 50.7 and 47.6 kHz , respectively. The aliphatic proton line (made up of contributions from the methylene groups in polyisoprene and in GLYMO as well as

the methyl groups in polyisoprene and in one of the minor hydrolysis products of GLYMO¹⁷) had two clear components: a broad component with a line width of 40 kHz and a narrower component with a line width of 8.3 kHz . The mobile component is naturally assigned to polyisoprene.

Determination of Domain Sizes by Spin Diffusion. The presence of significant dynamic heterogeneity in the lamellar composite suggests the possibility of using differences in mobility as a way to selectively excite magnetization in certain regions of the composite. More specifically, one could apply a “mobility filter” to suppress the signal from the less mobile spins and then monitor the diffusion of magnetization from the mobile to the immobile regions of the sample. Since the rate of spin diffusion is related to internuclear distances, such experiments allow the length scales in the sample to be determined.²⁷

Figure 3b shows a schematic of the ^{13}C -detected spin-diffusion NMR experiment used in this paper. The experiment consists of four basic steps: (1) a dipolar filter step which suppresses the ^1H magnetization of rigid parts of the sample, (2) a “mixing” step (characterized by a time, t_m) in which the remaining magnetization spreads to neighboring spins, (3) a transfer step in which ^1H magnetization is transferred to the nearest ^{13}C spins, and (4) a detection period in which resolved ^{13}C signals are recorded.

Figure 4b shows ^1H MAS spectra of the lamellar composite at 268 K recorded with and without application of the dipolar filter. In the spectrum without the filter, the broad signal due to the rigid PEO and GLYMO moieties can clearly be seen. In the spectrum with the filter, the effectiveness of the filter in removing the signal from rigid regions of the sample is manifested in a flattening of the baseline and a deepening of the “notch”. Due to T_2 relaxation during the multiple filter cycles, some of the polyisoprene signal is necessarily lost as well. Nonetheless, it is clear that the PEO and GLYMO signals have been completely suppressed. Thus, at the start of the mixing period, only polyisoprene protons have a net magnetization.

During the mixing time, this magnetization is transferred at a rate proportional to $1/r_{ij}^3$ (in abundant proton spin systems) by a process known as “spin diffusion”. At short mixing times, polarization is only transferred to spins near the magnetization source; at longer times, relayed transfer can occur. After the mixing period, a short cross-polarization step is used to monitor the location of the magnetization that has “diffused” throughout the sample.

Figure 11a shows the intensity of the $-\text{Si}-\text{CH}_2-$ carbon peak in the lamellar sample as a function of mixing time. The intensities were corrected for proton T_1 relaxation during the mixing time by multiplying each point by the factor e^{+t_m/T_1} where $T_1(268\text{ K}) = 1.5\text{ s}$ (as measured by inversion–recovery experiments). The initial rate of buildup is proportional to $\sqrt{t_m}$ as expected for spin-diffusion experiments.^{27,28} Intensities were normalized to the plateau value (the average of the last six data points). A linear fit to the first eleven data points gave a slope of $0.12 \pm 0.01\text{ ms}^{-1/2}$ and a y-intercept of 0.0 ± 0.04 . From these values, the x-intercept was found to be $0.0 \pm 0.5\text{ ms}^{1/2}$. The fact that the line extrapolates to the origin indicates that no significant PEO interphase is present, as will be explained below.

To check the consistency of these results, proton-detected spin-diffusion measurements were also carried out. Figure 11b shows the decay of the polyisoprene signal (estimated by taking the highest intensity point in the proton spectrum at 268 K ; see Figure 4b) as a function of $\sqrt{t_m}$. These values were corrected for T_1 relaxation using the multiplicative factor e^{+t_m/T_1} , and the

(39) *Polymer Handbook*, 3rd ed.; Brandrup, J., Immergut, E. H., Eds.; John Wiley and Sons: New York, 1989.

y-axis was scaled such that the y-intercept for the initial linear decay equaled 1.0. The slope of a line fit to the first six points was found to be $-0.115 \pm 0.004 \text{ ms}^{-1/2}$, which agrees remarkably well with the ^{13}C data.

Finally, proton T_2 's were measured by performing a series of spin-echo experiments on the lamellar composite at 280 K. This temperature was chosen because the static line width was equivalent to the MAS line width for the experiments performed at 268 K, and T_2 's cannot be measured on spinning samples. The total intensities were fit to a biexponential function of the form:

$$A_{\text{rigid}} \exp(-t/T_2^{\text{rigid}}) + A_{\text{mobile}} \exp(-t/T_2^{\text{mobile}})$$

with $A_{\text{rigid}} = 0.6 \pm 0.3$, $T_2^{\text{rigid}} = 220 \pm 80 \mu\text{s}$, $A_{\text{mobile}} = 0.4 \pm 0.4$, and $T_2^{\text{mobile}} = 700 \pm 300 \mu\text{s}$. These T_2 's can be considered crude approximations of the relative mobilities in the MAS experiment and can be used to estimate spin-diffusion constants.⁴⁰

Discussion

Phase Separation. The characteristics of an organic-inorganic composite are often determined by the nature of the interfaces in the material. Properties such as domain size, surface area, glass transition temperature, refractive index, and elasticity are all influenced by the specific interactions between the individual components.²

Frequently, hybrid materials are categorized by the nature of the interface between the inorganic and organic components. Class I hybrids are only held together by weak bonds, while class II hybrids have covalent connections.² Since the precursor GLYMO already contains a silicon-carbon bond, the hybrid materials studied in this paper necessarily belong to class II. However, the interface on which we want to focus in this study is not that between silicon and carbon atoms but rather that between the aluminosilicate-containing network (which also has organic components) and the purely organic block copolymer. Furthermore, in contrast to conventional templated^{4,5} and intercalated¹² systems, where the two components meet only at a well-defined interface, the GLYMO significantly penetrates the PEO phase of the block copolymer.¹³

The purpose of this study was to characterize the distribution of the GLYMO in the PEO phase. As mentioned in the Introduction, two possible scenarios can be envisioned: in one, the GLYMO is localized in the center of the PEO phase (see Figure 2a), and in the second, the GLYMO is distributed throughout the PEO block (see Figure 2b). Hydrogen bonds likely link these two components,^{10,17} but the extent of interpenetration is not apparent a priori. If entropic effects dominate, the PEO will significantly penetrate the aluminosilicate network. However, if this is not the case, an interphase of pure PEO could be expected to lie between the PI phase and the GLYMO-rich phase.

Structure of the Inorganic Components. The one-dimensional ^{27}Al and ^{29}Si NMR experiments (see Table 1) indicate that local inorganic environments in the composite materials do not change as a function of the ratio of inorganic to organic constituents. During the synthesis of the hybrid series, various amounts of the hydrolyzed aluminosilicate were mixed with the block copolymer and subjected to a heat treatment (1 h at 323 K followed by 1 h under vacuum at 403 K) to promote rapid alkoxide condensation.¹³ This heat treatment is also thought to

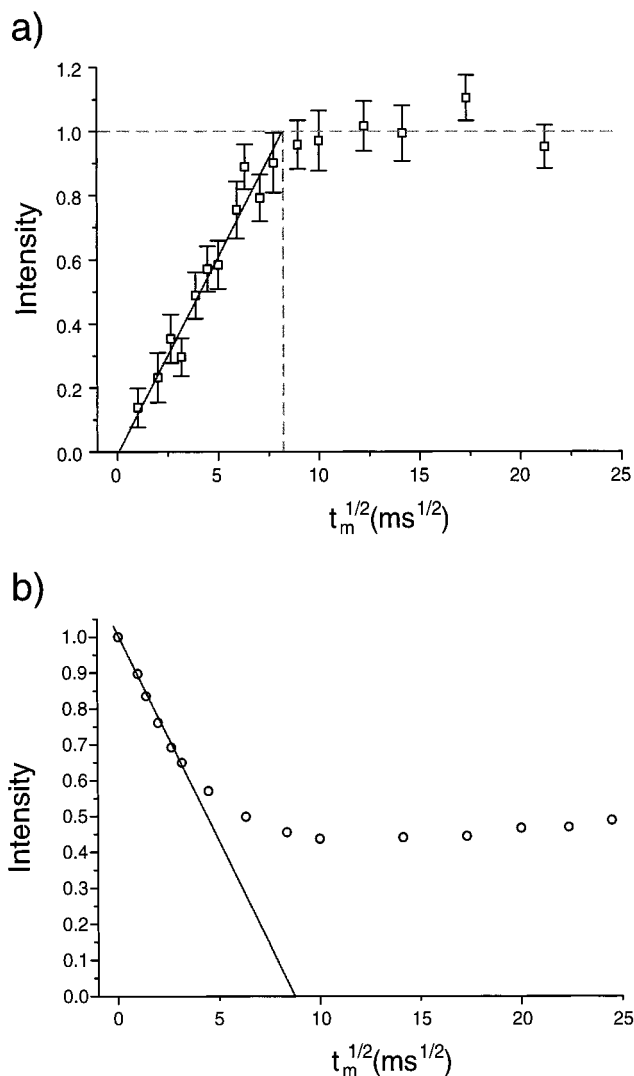


Figure 11. (a) Intensity of the signal from the carbon adjacent to silicon as a function of the square root of the mixing time after application of the pulse sequence of Figure 3b to the lamellar sample at 268 K. The solid line drawn through the data represents the best fit to the initial eleven points. The slope of this line is $0.12 \pm 0.01 \text{ ms}^{-1/2}$ and the x-intercept is $0.0 \pm 0.5 \text{ ms}^{1/2}$, indicating that there is no significant interphase between the polyisoprene and the inorganic portion of the composite. The error bars represent the root-mean-square of the noise for each spectrum. (b) Intensity of the signal from the polyisoprene protons as a function of the square root of the mixing time after application of the same dipolar filter as in part (a), followed by a mixing time and ^1H detection (no CP). The line drawn through the data represents the best fit to the initial six points. The decay of the polyisoprene signal occurs on the same time scale as the buildup of the signal at the carbon adjacent to silicon, confirming that PI is the source for spin diffusion.

facilitate mixing of the PEO and the aluminosilicate.¹³ However, the polymer does not appear to play much of a role in the inorganic network formation since the relative populations of the different silicon T-sites in hybrids do not differ from those in the pure hydrolyzed GLYMO/aluminum-*sec*-butoxide mixture. In contrast, the aluminosilicate network structure is strongly influenced by the ratio of GLYMO to aluminum *sec*-butoxide, by the presence or absence of additives, and by whether the hardening process occurs under vacuum or at atmospheric pressure.⁴¹ It is likely, therefore, that the aluminosilicate network

(40) Mellinger, F. Ph.D. Thesis, Johannes Gutenberg University, Mainz, Germany, 1998.

(41) Templin, M. Ph.D. Thesis, Johannes Gutenberg University, Mainz, Germany, 1998.

already starts to form before addition of the block copolymer and that the subsequent heat treatment promotes entropic mixing of the PEO and GLYMO chains.

The local inorganic environments are also largely unaffected by geometric constraints. Approximately the same relative site populations are observed when the inorganic network is confined to 12-nm diameter spheres¹⁵ as when it is in the bulk. Thus, addition of aluminosilicate to the block copolymer has the primary effect of “swelling” the PEO phase without causing substantial alteration of the inorganic network itself.

Dynamics of the Organic Components. Additional information about the interactions between GLYMO and PEO is provided by WISE and DSC measurements. The two-dimensional WISE experiment (see Figure 10) indicates the presence of significant dynamical heterogeneity in the composite materials. In particular, the polyisoprene is quite mobile, while both the PEO and GLYMO phases are significantly more rigid. The glass transition of PI (as measured by DSC) is, in fact, the same in the composites as in the pure block copolymer ($T_g \approx 214$ K) and well below the temperature at which the experiments were performed. However, the behavior of the PEO phase is dramatically different in the composites as compared to that in the bulk block copolymer. While the pure block copolymer shows a strong melting peak (see Figure 9a), crystallization of PEO is entirely suppressed in the composites (see Figure 9b). This provides evidence for significant mixing of the inorganic and PEO phases. Note that composites with higher PEO volume fractions (up to 35%) also fail to show a melting peak.^{13,42}

Interface between Organic/Inorganic Hybrid and Organic Regions. The results of the carbon-detected spin-diffusion experiments (presented in Figure 11a) demonstrate that no significant PEO interphase is present between the mobile polyisoprene and the immobile inorganic phase in the lamellar composite. This can be seen from the fact that the initial buildup of the curve extrapolates to an x -intercept of zero.^{24,34} From the two-dimensional WISE experiments, we know that the PEO is immobile and, therefore, its magnetization is suppressed by the dipolar filter. If there were a PEO interphase (see Figure 2a), magnetization would initially diffuse from the polyisoprene to this PEO phase. Only at later times would it reach the GLYMO protons. Such a situation would correspond to a spin-diffusion buildup plot for the GLYMO carbon which has an x -intercept that is greater than zero. The absence of such a “lag time” in Figure 11 indicates that the model of Figure 2b, where PEO and GLYMO are intimately mixed, is representative of our system.

Due to the fact that the spin-diffusion results, like all measurements, are subject to experimental error, one cannot rule out the possibility of the presence of a small interfacial layer of PEO in the lamellar composite. However, it is possible to estimate an upper bound for such a layer. From the linear fit to the first 11 points of the spin-diffusion buildup curve (see Figure 11a), the x -intercept was determined to be 0.0 ± 0.5 ms^{1/2}. Using the simple approximation that the mean-square displacement for a diffusive process is given by $\langle x^2 \rangle = 6Dt$ and that the spin diffusion constant for rigid samples is typically $D = 0.8$ nm²/s,²⁷ an error bar of 0.5 ms^{1/2} would correspond to a length scale of 1 nm. Thus, 10 Å may be considered to be a reasonable upper bound for the size of a region rich in PEO segments. Since the results of small-angle X-ray scattering (SAXS)¹⁵ combined with transmission electron microscopy (TEM) measurements⁴² indicate that the PEO/GLYMO/aluminum-*sec*-bu-

toxide layers are 9 nm thick, a 1-nm layer would still be quite small, and the model of Figure 2b is still a much better description of the system than that of Figure 2a. Note that 1 nm is also significantly smaller than the mean squared end-to-end distance of a freely rotating chain of PEO ($\langle r^2 \rangle_{0f}^{1/2} = 2.3$ nm for $M_n(\text{PEO}) = 1800$ g/mol),³⁹ which can be taken to represent a lower bound for the size of a PEO-rich interphase if the model of Figure 2a were correct.

The proton-detected spin-diffusion measurements of Figure 11b demonstrate that the decay of the polyisoprene signal occurs on the same time scale as the buildup of the GLYMO signal in Figure 11a. This nicely confirms that spin diffusion from PI to GLYMO is responsible for the observed changes in intensity in Figure 11a. Although analysis of spin-diffusion decay (rather than buildup) curves generally has the advantage that domain sizes can be estimated without including stoichiometric factors,⁴³ decay curves cannot address the issue of whether an interphase is present. Furthermore, the partial overlap of PI and PEO signals in our system (see Figure 4b) prevents a quantitative analysis of the proton-detected data. However, the ¹³C-detected data (Figure 11a) should be quantitatively correct since the peak at 10.2 ppm does not overlap with any signals from the polymer.

Thickness of Phase-Separated Lamellae. As a further check on the accuracy of the spin-diffusion experiment, one can compare the long period of the lamellae as deduced from the spin-diffusion data with that determined independently from SAXS experiments. For a lamellar system composed of alternating mobile and immobile regions, the thickness of the lamellae which contain mobile species is given by

$$d_{\text{mobile}} = \frac{V^{\text{total}}}{V^{\text{rigid}}} \sqrt{\frac{4D_{\text{eff}} t_m^s}{\pi}} \quad (1)$$

where $\sqrt{t_m^s}$ is the value of the square root of the mixing time at the point where the line corresponding to the initial linear buildup extrapolates to the plateau value.²⁷ For the data in Figure 11a, $\sqrt{t_m^s}$ equals 8.3 ms^{1/2}. The diffusion constant for a two-component system is given by

$$\sqrt{D_{\text{eff}}} = \frac{\sqrt{D_{\text{mobile}} D_{\text{rigid}}}}{(\sqrt{D_{\text{mobile}}} + \sqrt{D_{\text{rigid}}})/2} \quad (2)$$

Unfortunately, D_{mobile} and D_{rigid} are difficult to determine a priori. Overlap of the mobile and rigid signals in the lamellar composite prevent T_{2D} 's for the different species⁴³ from being directly measured. However, values can be estimated by fitting the T_2 -decay curve for the entire sample (obtained from a series of Hahn echo experiments) to a biexponential function and identifying the rapidly decaying component with the rigid part of the sample and the slowly decaying component with the mobile part. These T_2 values, in turn, can be related to diffusion constants using previously established empirical correlations.^{40,44}

Since lamellae necessarily share a common surface, the volume fraction appearing in eq 1 reduces to a ratio of distances. Solving for the length of the long period, L , in terms of the ratios d_{mobile}/L and d_{rigid}/L gives

(43) Mellinger, F.; Wilhelm, M.; Landfester, K.; Spiess, H. W.; Haunschuld, A.; Packusch, J. *Acta Polym.* **1998**, *49*, 108.

(44) Diffusion constants were estimated according to the formula $D = 0.00017/(\pi T_2) + 0.22$. This empirical correlation was established for T_2 's in the range 300 μ s to 1 ms.⁴⁰ The T_2 value for PEO in the lamellar sample falls outside this range. Nonetheless, we have used this relation as a rough approximation.

(42) Ulrich, R.; Du Chesne, A.; Templin, M.; Wiesner, U., unpublished results.

$$L^{\text{NMR}} = \left[\frac{d_{\text{mobile}}}{L} \frac{d_{\text{rigid}}}{L} \right]^{-1} \sqrt{\frac{4D_{\text{eff}}^s}{\pi}} \quad (3)$$

Using the values for D_{eff} and $\sqrt{r_m^s}$ determined above gives $L^{\text{NMR}} = 23.8$ nm when the ratios d_{mobile}/L and d_{rigid}/L are determined from TEM and $L^{\text{NMR}} = 23.0$ nm when the ratios are determined from volume fractions of the reactants.⁴² In contrast, SAXS experiments give $L^{\text{SAXS}} = 22.0$ nm.¹⁵ Given the crudeness of the approximations involved, this agreement is quite reasonable, and the spin-diffusion results appear consistent with SAXS measurements.

We also attempted to perform the spin-diffusion experiment of Figure 3b using ^{29}Si detection instead of ^{13}C detection in order to see if certain types of T^n sites in the organosilicate network were preferentially located nearer to the interface than others. Unfortunately, the large width of the ^{29}Si spectrum (see Figure 7) makes the signal-to-noise too poor to allow the experiment to be performed on a reasonable time scale.

Although the NMR results clearly suggest that some of the GLYMO is located near the PI/PEO interface, it is not possible to distinguish between models (originally proposed for addition of low molecular weight homopolymers to block copolymers) in which the distribution of the aluminosilicate is nearly uniform throughout the entire layer²⁰ and those in which a significant amount is located at the edges but a slight preference for the center is still observed.⁴⁵ Given the fact that the molar fraction of PEO in the PEO/aluminosilicate layer is only 0.31, it is possible that a GLYMO-rich region is present in the center of the block. Nonetheless, it is clear that the aluminosilicate network behaves qualitatively more like a low molecular weight homopolymer than a high molecular weight homopolymer.

Comparison with Related Systems. It is interesting to compare these results with recent studies of block copolymer/epoxy resin composites.^{18,19} In these studies, low molecular weight epoxy resins are shown to selectively swell the PEO phase of an amphiphilic block copolymer (either poly(ethylene-oxide-*b*-ethyl-ethylene) or poly(ethylene-oxide-*b*-ethylene-*alt*-propylene)). As in the case of the aluminosilicate/PI-*b*-PEO composite, a series of ordered phases can be produced, and the phase diagram can be understood by analogy to block copolymer/homopolymer blends.¹⁹ Upon curing, however, the PEO is locally expelled from the epoxy matrix, producing an interphase region of pure PEO, which can be observed directly in transmission electron micrographs.¹⁸ Supporting evidence for the existence of a pure PEO interphase comes from DSC measurements which show that crystalline PEO regions are present in the cured composite. The expulsion of the PEO can

be attributed in part to the increased molecular weight of the cured epoxy polymer.¹⁹

In contrast, the addition of the aluminosilicate to the PI-*b*-PEO block copolymer leads to an intimate mixture of the PEO and the inorganic component. Both NMR and DSC measurements indicate that a PEO interphase is not established. Thus, the inorganic network does not expel the PEO but rather behaves like a low molecular weight homopolymer under our experimental conditions. The GLYMO and the PEO are intrinsically compatible.

The compatibility of the aluminosilicate network with one phase of the block copolymer has intriguing implications for the development of new materials. In contrast to conventional templated composites where the surfactants can be washed away to leave a purely inorganic network,⁴⁻⁶ dissolution of the PI-*b*-PEO/aluminosilicate composites has been shown to lead to separated spheres, cylinders, or plates of *hybrid* material.¹⁵ Each of these "hairy nano-objects" consists of an aluminosilicate core surrounded by a thin polymer layer, and the intrinsic compatibility of PEO and GLYMO is what keeps the polymer tethered to the inorganic network. The effects of the intimate mixing between the polymer chains and the inorganic network on the mechanical properties of such hybrid materials still need to be elucidated. However, such materials could potentially find application, e.g., as polymer reinforcing agents.

Conclusions

By applying a variety of solid-state NMR techniques, we have shown that a hydrolyzed GLYMO/aluminum-*sec*-butoxide mixture is intrinsically compatible with PEO. In hybrid materials formed from this aluminosilicate and PI-*b*-PEO block copolymer, no evidence for a PEO interphase between the inorganic hybrid and the organic PI phase was observed by either spin-diffusion NMR studies or DSC measurements. This suggests that entropic effects drive the mixing of the aluminosilicate with the PEO. Despite the extent of this mixing, one-dimensional NMR spectra indicate that the local inorganic environments are not significantly perturbed by the incorporation of the aluminosilicate network into the block copolymer. The presence of the block copolymer appears to have a negligible effect on the alkoxide condensation process. However, addition of the inorganic component to the block copolymer prevents PEO crystallization, and WISE NMR experiments show that the PEO/aluminosilicate phases in the hybrids with a significant aluminosilicate fraction are uniformly rigid.

Acknowledgment. S.M.D. thanks the National Science Foundation of the United States for an NSF-NATO postdoctoral fellowship. J.W.Z. gratefully acknowledges an Alexander-von-Humboldt Research Fellowship. The authors thank Drs. Manfred Wilhelm, Markus Templin, and Felix Mellinger for helpful discussions and are grateful to the Bundesministerium für Bildung und Forschung for financial support.

JA984389Q

(45) Winey, K. I.; Thomas, E. L.; Fetters, L. J. *Macromolecules* **1991**, *24*, 6182.

(46) Pham, Q. T.; Pétiard, R.; Waton, H.; Llauro-Darricades, M.-F. *Proton and Carbon NMR Spectra of Polymers*; Penton Press: London, 1991.

(47) Langer, B.; Schnell, I.; Spiess, H. W.; Grimmer, A.-R. *J. Magn. Reson.* **1999**, *138*, 182.